New Phytologist

Research

Compartment-specific Ca^{2+} imaging in the green alga *Chlamydomonas reinhardtii* reveals high light-induced chloroplast Ca^{2+} signatures

Matteo Pivato[1], Matteo Grenzi[2], Alex Costa[2,3] and Matteo Ballottari[1]

[1]Department of Biotechnology, University of Verona, Strada le Grazie 15, 37134, Verona, Italy; [2]Department of Biosciences, University of Milan, Via Giovanni Celoria 26, 20133, Milan, Italy; [3]Institute of Biophysics, National Research Council of Italy (CNR), Milan, 20133, Italy

Author for correspondence:
Matteo Ballottari
Email: matteo.ballottari@univr.it

Received: *31 May 2023*
Accepted: *26 June 2023*

New Phytologist (2023)
doi: 10.1111/nph.19142

Key words: calcium, cell signaling, Chlamydomonas, chloroplast, photoreceptor, photosynthesis, reactive oxygen species, single-cell imaging.

Summary

- To investigate the role of intracellular Ca^{2+} signaling in the perception and response mechanisms to light in unicellular microalgae, the genetically encoded ratiometric Ca^{2+} indicator Yellow Cameleon (YC3.6) was expressed in the model organism for green algae *Chlamydomonas reinhardtii*, targeted to cytosol, chloroplast, and mitochondria.
- Through *in vivo* single-cell confocal microscopy imaging, light-induced Ca^{2+} signaling was investigated in different conditions and different genotypes, including the photoreceptors mutants *phot* and *acry*. A genetically encoded H_2O_2 sensor was also adopted to investigate the possible role of H_2O_2 formation in light-dependent Ca^{2+} signaling.
- Light-dependent Ca^{2+} response was observed in *Chlamydomonas reinhardtii* cells only in the chloroplast as an organelle-autonomous response, influenced by light intensity and photosynthetic electron transport. The absence of blue and red-light photoreceptor aCRY strongly reduced the light-dependent chloroplast Ca^{2+} response, while the absence of the blue photoreceptor PHOT had no significant effects. A correlation between high light-induced chloroplast H_2O_2 gradients and Ca^{2+} transients was drawn, supported by H_2O_2-induced chloroplast Ca^{2+} transients in the dark.
- In conclusion, different triggers are involved in the light-induced chloroplast Ca^{2+} signaling as saturation of the photosynthetic electron transport, H_2O_2 formation, and aCRY-dependent light perception.

Introduction

Growth and survival of living organisms depend on their ability to sense the environmental conditions and respond to external stimuli. In plants, calcium (Ca^{2+})-dependent signaling plays a well-characterized role in the perception and response mechanisms to a great variety of environmental stresses, including temperature fluctuations, drought, salinity, pathogen attack, and mechanical stimulation (Dodd *et al.*, 2010; Kudla *et al.*, 2018). Some of these response mechanisms are conserved among unicellular microalgae, a large and diverse group of photosynthetic eukaryotes, where Ca^{2+} is a crucial second messenger and a key player in signal transduction pathways (Edel *et al.*, 2017). In the green model alga *Chlamydomonas reinhardtii*, Ca^{2+} signaling has been described in many motile responses, in stress responses to environmental stimuli, bacterial toxins and also in the regulation of photosynthesis (Wakabayashi *et al.*, 2009; Petroutsos *et al.*, 2011; Bickerton *et al.*, 2016; Rose *et al.*, 2021; Hou *et al.*, 2023). Many of these signal transduction pathways, however, still need to be characterized, and our knowledge on Ca^{2+} signaling mechanisms in green algae remains limited.

Upon perception of specific environmental stimuli, the interplay between Ca^{2+} influx and efflux pathways rapidly changes within the cell; this consequently modulates the cytosolic Ca^{2+} concentrations ($[Ca^{2+}]_{cyt}$) and causes Ca^{2+} binding-induced conformational changes in a specific set of proteins, finally leading to the downstream activation of consequent biological processes (Edel *et al.*, 2017). Uptake and extrusion of Ca^{2+} across biological membranes is favored by Ca^{2+}-permeable channels, Ca^{2+} transporters, and pumps (Demidchik *et al.*, 2018; Resentini *et al.*, 2021b). Ca^{2+}-decoding 'tools' instead are represented by Ca^{2+}-binding sensor proteins (Kudla *et al.*, 2018). These molecules are part of the Ca^{2+} signaling toolkit, that in unicellular microalgae is characterized by a surprising diversity, differing significantly from both land plants and animal counterparts (Verret *et al.*, 2010). *C. reinhardtii* Ca^{2+} signaling toolkit, in particular, presents several unique elements (i.e. channelrhodopsins, ChRs), accompanied by other Ca^{2+}-related molecular players conserved among *Viridiplantae* and other 'animal-like' Ca^{2+} signaling components (Pivato & Ballottari, 2021).

Ca^{2+} signaling mechanisms have also evolved at the endomembrane level, exploiting intracellular organelles as Ca^{2+} storage

compartments, as in the case of the apoplast/cell wall, vacuole, and the endoplasmic reticulum (Resentini *et al.*, 2021a,b), but also as compartments able to generate their own intraorganellar Ca^{2+} signals, as in the case of chloroplasts, mitochondria, and the nucleus (Stael *et al.*, 2012; Costa *et al.*, 2018; Pirayesh *et al.*, 2021).

Chloroplasts have long been known to be involved in the shaping of intracellular Ca^{2+} signaling and homeostasis (Navazio *et al.*, 2020). In plants, imaging analysis using the bioluminescent Ca^{2+} reporter aequorin or fluorescent Förster Resonance Energy Transfer (FRET)-based Ca^{2+} reporter proteins revealed specific chloroplast Ca^{2+} signals in response to elicitors of plant defense responses, cold, heat, oxidative, salt, and osmotic stresses (Nomura *et al.*, 2012; Loro *et al.*, 2016; Sello *et al.*, 2016, 2018; Lenzoni & Knight, 2019; Navazio *et al.*, 2020; Volkner *et al.*, 2021). Changes in free [Ca^{2+}] are reported to modulate crucial aspects of photosynthesis, including the assembly and function of PSII, the regulation of stromal enzymes of the Calvin cycle, as well as stomatal movements, chloroplast import of nuclear-encoded proteins, or photoacclimation (Rocha & Vothknecht, 2012; Hochmal *et al.*, 2015). In *C. reinhardtii*, Ca^{2+} is involved also in the high light induction of the major protein necessary for the regulation of the photoprotective mechanism of nonphotochemical quenching (NPQ), LHCSR3, which requires the Ca^{2+}-sensing protein CaS (Petroutsos *et al.*, 2011). Moreover, cellular Ca^{2+} homeostasis was reported to provide a fine-tuning modulation of cyclic photosynthetic electron flow (CEF) under anaerobic conditions in a CaS-dependent manner, thereby regulating photosynthetic electron transfer (Terashima *et al.*, 2012).

Light has been shown to modulate plant chloroplast [Ca^{2+}], affecting Ca^{2+} fluxes and causing an increase of stromal [Ca^{2+}] upon dark transition (Sai & Johnson, 2002; Nomura *et al.*, 2012; Sello *et al.*, 2016, 2018). This rise of stromal [Ca^{2+}] has been suggested to act as a post-translational regulator of the activity of some Calvin cycle enzymes, resulting in a further inhibition of CO_2 fixation during the night (Sai & Johnson, 2002). The circadian gating of dark-induced chloroplast and cytosolic Ca^{2+} elevations has recently been demonstrated (Martí Ruiz *et al.*, 2020); however, the molecular mechanisms underlying chloroplast dark-induced Ca^{2+} fluxes remain to be unraveled. Moreover, many studies have focused on the physiological response to low light or to light-to-dark transition, but photosynthetic organisms within their natural habitats can also experience high light illumination or rapid changes in solar irradiance (sun flecks). Under these conditions, the supply of light energy could exceed the dissipation capacity of the photosynthetic machinery, leading to the photoreduction of O_2 and to the formation of reactive oxygen species (ROS; Erickson *et al.*, 2015). The accumulation of ROS can oxidatively damage macromolecules, and some of the released oxidation products, as oxylipins, can act as signaling molecules and mediate cell responses to biotic and abiotic stresses. Nevertheless, some ROS have also been proposed as direct signaling molecules, triggering cell adaptation and mitigating the risk of oxidative stress (Suzuki *et al.*, 2012). Among the different ROS molecules, the longer half-life of H_2O_2 and its ability to permeate cell membranes through aquaporins make this molecule the most likely ROS involved in cell signaling events. The interplay between Ca^{2+}- and ROS-mediated signaling events has also been described in several responses to endogenous and environmental stimuli in plants (Choi *et al.*, 2016).

Chlamydomonas reinhardtii has been widely exploited as a model organism to study redox regulation and ROS signaling (Wakao & Niyogi, 2021): Here, light can be perceived by a specific network of photoreceptors, including a phototropin (PHOT), four cryptochromes (one animal-type, aCRY, one plant cryptochrome, pCRY, and two DASH cryptochromes), two channelrhodopsins (ChR1 and ChR2) and eight histidine-kinase rhodopsins, as well as the UV-B photoreceptor UVR8 (Greiner *et al.*, 2017; Petroutsos, 2017). The role of most of these proteins in *Chlamydomonas* cell physiology has been unraveled in recent works, indicating PHOT as a blue-light photoreceptor essential in the feedback regulation of photosynthesis and photoprotection, and aCRY as a blue-light photoreceptor that can respond also to red or yellow light (Beel *et al.*, 2012; Petroutsos *et al.*, 2016). The functional characterization of aCRY through an insertional *acry* mutant showed a significantly lower induction of the transcript levels of several genes of chlorophyll and carotenoid biosynthesis, light-harvesting complexes, nitrogen metabolism, the cell cycle, and the circadian clock in response to blue and red light (Beel *et al.*, 2012). A recent work showed indeed that aCRY plays also a key role in different steps of gametogenesis and zygote germination (Zou *et al.*, 2017); however, its role in the regulation of light perception and harvesting still remains elusive.

Here, we report the establishment of different Yellow Cameleon (YC3.6; Nagai *et al.*, 2004) *C. reinhardtii* lines, expressing the Ca^{2+} FRET-based biosensor at the level of specific subcellular compartments: cytosol, mitochondrial matrix, and chloroplast stroma, as a tool to explore the characteristics of intracellular Ca^{2+} dynamics. We apply *in vivo* single-cell imaging techniques to study *C. reinhardtii* light-dependent Ca^{2+} signaling at subcellular resolution. Through this approach, we report chloroplast blue and red light-induced [Ca^{2+}] transients, characterized by stimulus-specific kinetic parameters. Moreover, we investigated the role in light-dependent Ca^{2+} signaling of photosynthetic activity, ROS production, and photoreceptors activity.

Materials and Methods

Algal strains and culture conditions

The *Chlamydomonas reinhardtii* Dangeard strains used in this study were UVM4 (UV-mediated mutant 4; Neupert *et al.*, 2009), *phot1* (CC-5392), CC-125 mt+, *acry*-A3 mt+ (CC-5396) and SAG73.72. *phot1* was kindly provided by Dr Dimitris Petroutsos (CNRS/CEA Grenoble), whereas *acry* was purchased from Chlamydomonas Resource Center (https://www.chlamycollection.org/). Transgenic roGFP2-Tsa2ΔC_R lines (Niemeyer *et al.*, 2021) were kindly provided by Prof. Michael Schroda (Molecular Biotechnology & Systems Biology, TU Kaiserslautern, Germany). Algal cells were cultivated in Tris-acetate-phosphate (TAP) or High Salts (HS) minimal medium (Harris, 2008; Kropat *et al.*, 2011). Liquid cultures were

maintained in shake flasks at 25°C and 70–100 µmol photons m^{-2} s^{-1} of continuous white light, unless otherwise stated. High light acclimation of photoautotrophically grown cells was performed for 15 d in shake flasks at 400 µmol photons m^{-2} s^{-1} of continuous white light. All the experiments herein reported were done on cells at exponential phase.

Chlamydomonas reinhardtii genetic transformation

The YC3.6 coding sequence (Nagai *et al.*, 2004; Yang *et al.*, 2008) was synthetically redesigned, to enhance transgene expression, by codon usage optimization and intron spreading, as recently described (Baier *et al.*, 2018). Synthetic YC3.6 nucleotide sequence (Thermo Scientific, Waltham, MA, USA) was cloned into pOptimized (pOpt2) vector backbone by *Nde*I-*Bgl*II sites (Lauersen *et al.*, 2015) using Hsp70A/Rbsc2 hybrid promoter obtaining the cytosolic localization of the probe. To respectively obtain chloroplast and mitochondrial subcellular localization of YC3.6 protein product, *C. reinhardtii* photosystem I subunit D (PsaD) and mitochondrial ATP synthase subunit A (AtpA) N-terminal targeting peptides were cloned at the N-terminus of YC3.6 cassette, through *Xba*I-*Bgl*II sites (Lauersen *et al.*, 2015). Strep-tag® II flag, a short peptide of eight amino acids (WSHPQFEK), was fused to the C-terminal of the protein in all the mentioned vectors. Two different antibiotic resistance genes, respectively for hygromycin (*aphVII*) or paromomycin (*aphVIII*), were used in this study for the selection of transformed strains (Lauersen *et al.*, 2015). Stable nuclear transformation was carried out by glass beads agitation, as described previously (Kindle, 1990), using 10 µg of linearized plasmid DNA. Transformant strain selection was performed on TAP agar plates supplied with antibiotics (12 µg ml^{-1} of paromomycin and 15 µg ml^{-1} for hygromycin), for 5–7 d at 200 µmol m^{-2} s^{-1} light intensity. Antibiotic-resistant colonies were picked to fresh plates and inoculated in 96-well microtiter plates with TAP medium, cultivating at 200 µmol m^{-2} s^{-1} light intensity until sufficiently dense. Selection of strains expressing *YC3.6* was done by measuring fluorescence emission at 520–560 nm upon excitation at 509 nm with an Infinite PRO 200 plate reader (Tecan, Mannedorf, Switzerland). Fluorescence emissions were normalized to 720 nm cell scattering of the same sample as a proxy of cell density.

Protein extraction and SDS-PAGE

Protein extracts were analyzed by SDS-PAGE as described in Laemmli (1970). Western blot analysis was performed using anti-GFP (Green Fluorescent Protein) antibody (Merck, Darmstadt, Germany) and an anti-rabbit Immunoglobulin G Alkaline Phosphatase-conjugated secondary antibody (Merck).

Confocal laser scanning microscopy and cells imaging

Confocal laser scanning microscopy (CLSM) analyses were performed using a TCS-SP5 inverted confocal microscope (Leica Microsystem, Wetzlar, Germany). Images were acquired by a 63× 1.40 NA oil immersion objective with different digital zoom. Ca^{2+} imaging of living cells was performed as described in Loro & Costa (2013). YC3.6 was excited at 458 nm, and emission of FRET pair proteins ECFP and cpVenus was collected at 475–505 nm and 525–545 nm, respectively, with two Hybrid spectral detectors. Laser light stimuli were administered by switching on the laser line (405 nm, 633 nm, or 514 nm) at the desired intensity. Laser incident power on sample was measured through a power meter, considering the specific objective transmission at the different wavelengths (Supporting Information Fig. S1). Tsa2ΔC_R fluorescence was measured as described in Morgan *et al.* (2011, 2016), with 405 and 488 nm excitations used sequentially with emission in the 500–530 nm range.

Mid/Late-log phase *C. reinhardtii* cell cultures were kept in light until the experiment, when they were placed into a home-made glass-bottomed chamber slide. The bottom of the chamber was coated with 0.01% poly-L-lysine (Merck) to facilitate adherence of the cells. All the experiments were done at room temperature (24°C). To test YC3.6 subcellular localization, cpVenus, and chlorophyll were excited, respectively, by the 514 nm and 633 nm laser lines, and the emission was collected, respectively, at 525–545 nm and 670–690 nm, with the pinhole set to 1 airy unit. Mitochondria were visualized using MitoLite™ Red CMXRos (AAT Bioquest, Pleasanton, CA, USA). For the latter, cultures were incubated for 30 min with MitoLite at a final concentration of 1 µM and then washed with fresh medium before imaging. MitoLite excitation/emission settings were 543 nm/590–620 nm HyD hybrid detector and collected sequentially and separately from those of cpVenus and chlorophyll to maximize the specificity of detection. Before measurements, steady-state FRET ratio was monitored by illuminating the cells by continuous laser light at 458 nm for 2 min to ensure signal stability. $CaCl_2$, H_2O_2, and DTT stimuli at different final concentrations were applied by direct injection of a 1000× stock solution into the imaging chamber. When required, 10 µm 3-(3,4-dichlorophenyl)-1, 1-dimethylurea (DCMU) and 2 µm 2,5-dibromo-6-isopropyl-3-methyl-1,4-benzoquinone (DBMIB) were added at to the samples at least 15 min before measurements. To assess whether extracellular Ca^{2+} is involved in chloroplast [Ca^{2+}] elevations in response to high light, 200 µM EGTA was added to the cells' external medium 10 min before measurements. Images were analyzed using ImageJ software. cpVenus and CFP emissions of the analyzed regions of interest were used for the FRET ratio calculation (cpVenus : CFP) and, where suitable, normalized to the initial ratio and plotted vs time. Background subtraction was performed independently for both channels before calculating the ratio. Maximal FRET ratio variation was calculated subtracting the median of the prestimulus FRET ratio values. In the case of RoGFP2-Tsa2ΔCR fluorescence background, subtraction was applied normalizing the values to the initial ratio and plotting vs time.

Measurement of photosynthetic activity

Photosynthetic parameters ΦPSII (yield of Photosystem II upon illumination), qL (indicating the redox state of plastoquinones), electron transport rate (ETR), and NPQ (indicating the

nonphotochemical quenching, being the quenching of the fluorescence emitting due to thermal dissipation of a fraction of the energy absorbed) were measured with a DUAL-PAM-100 fluorimeter (Heinz–Walz) on dark-adapted intact cells, at room temperature in a 1 × 1 cm cuvette, according to van Kooten & Snel (1990) and Baker (2008). The different intensities of the actinic light used were reported in the different cases.

Spectroscopy and pigment content analysis

Pigments were extracted from intact cells using 80% acetone buffered with Na_2CO_3 and their absorption spectra analyzed as described previously (Croce *et al.*, 2002).

Statistical analysis

Student's two-tailed *t*-test or one-way ANOVA for independent samples were applied to statistically evaluate results as reported in the figure legends. Error bars indicate SD. The number of independent biological replicates used to calculate SD is indicated in the figure legends.

Results

Expression and targeting of YC3.6 indicator to different *Chlamydomonas reinhardtii* subcellular compartments

To obtain *C. reinhardtii* lines stably transformed with the Ca^{2+} sensor Yellow Cameleon (YC3.6), smart synthetic gene design strategy was applied to optimize nuclear transgene expression (Baier *et al.*, 2018). YC3.6 sensor was expressed in UVM4 strain, previously selected for efficient expression of nuclear transgenes (Neupert *et al.*, 2009), with cytosolic, chloroplast, and mitochondrial localization (Fig. 1a): For each subcellular localization, 96 transformed colonies grown on selective plates were screened for cpVenus fluorescence, selecting for subsequent analysis the two lines showing the highest fluorescence. The accumulation of YC3.6 protein was confirmed in the transgenic lines by western blot analysis (Fig. 1b). The subcellular localization of accumulated protein into the three different compartments was confirmed by confocal microscopy for the transgenic lines selected using chlorophyll and MitoTracker MitoLite™ Red CMXRos fluorescence to visualize respectively chloroplasts and mitochondria (Fig. 1c). Immunotitration analysis revealed a significantly lower accumulation of the YC3.6 in the cells expressing the chloroplast and mitochondrial localized probes (Fig. S2). However, ratiometric Ca^{2+} probes as YC3.6 rely completely on ratio changes to monitor [Ca^{2+}]; thus, the obtained measurements are not influenced by the actual amount of the indicator or by changes in the focusing position of the imaging system (Grenzi *et al.*, 2021). Potential effects of YC3.6 protein accumulation on *C. reinhardtii* photosynthetic performance were also tested by measuring photosystem II (PSII) maximum quantum efficiency (PSIIΦ) in dark-adapted cells, showing no significant differences between the transgenic lines and wild-type (Fig. S2).

To investigate the functionality of the YC3.6 probe *in vivo* in *C. reinhardtii* cells, we performed a series of Ca^{2+} imaging analyses at single-cell resolution. Previous works demonstrated how Ca^{2+}-dependent signaling pathways in *C. reinhardtii* can be influenced by the concentration of external Ca^{2+} in the medium (Quarmby & Hartzell, 1994; Petroutsos *et al.*, 2011). Cell cultures previously depleted of external Ca^{2+} (three consecutive washing steps with -Ca^{2+} medium) were thus exposed to different $CaCl_2$ concentrations, exhibiting increased FRET ratios due to [Ca^{2+}] elevations at the level of all the three different subcellular compartments where YC3.6 is expressed (cytosol, chloroplast stroma, and mitochondrial matrix; Fig. S3), even if with different dynamics and kinetic parameters. Similarly, previous works reported that the rapid addition of 20 mM external Ca^{2+} to *C. reinhardtii* cells causes cytosolic [Ca^{2+}] elevations (Wheeler *et al.*, 2007; Wheeler, 2017). It is worth noting that the application of high extracellular $CaCl_2$ concentrations may cause a hyper-osmotic shock, with ionic and osmotic components, that could trigger [Ca^{2+}] transients. Salt stress, in fact, triggers cytosolic [Ca^{2+}] elevations in *C. reinhardtii* and both a cytosolic and chloroplast [Ca^{2+}] elevation in plant cells (Bickerton *et al.*, 2016; Sello *et al.*, 2016). YC3.6 probe efficiently reported Ca^{2+} dynamics at the level of all the three different compartments; however, at this point of the analysis, we cannot assess whether the [Ca^{2+}] elevation was triggered because of the sensing of the high extracellular [Ca^{2+}] itself or as a response to the hyper-osmotic shock.

Subcellular Ca^{2+} monitoring reveals high light-induced chloroplast-specific Ca^{2+} elevations

Ca^{2+} imaging analyses on YC3.6 expressing lines were performed subsequently in response to a light stimulus. The 633 nm and 405 nm laser lines of the confocal microscope used to perform Ca^{2+} imaging in single cells were used to apply 90 s of respectively 5 s^{-1} pulsed red or blue light directly to *C. reinhardtii* cells, while monitoring [Ca^{2+}] at the level of each specific subcellular compartment. Exciting the cells with a laser light caused a slight change in the FRET ratio during the stimulus onset in all the three tested compartments, positive when stimulated with the 633 nm line and negative with the 405 nm line (Fig. 2a–c). The high-intensity illumination might transiently influence YC3.6 emission properties during the stimulation phase, without affecting its functionality. The 405 nm line, for instance, could preferentially excite the CFP moiety of the YC3.6 probe, resulting in a negative change in the FRET ratio. When the light stimulus was switched off, however, the FRET ratio change in the case of YC3.6 probe localized in the cytosol or mitochondria compartments was close to zero, indicating no alteration of the [Ca^{2+}]. Differently, the lines expressing YC3.6 probe in the chloroplast showed a significantly higher transient [Ca^{2+}] elevation, characterized by *bona fide* FRET responses (Figs 2b,d, S4). Interestingly, we found that both the tested laser wavelengths induced chloroplast-specific [Ca^{2+}] transients, with similar dynamic and kinetic parameters (Fig. 2). The same light stimuli, however, did not induce [Ca^{2+}] elevations at the level of the cytosolic or mitochondrial compartments (Fig. 2a,c). Similarly, green light

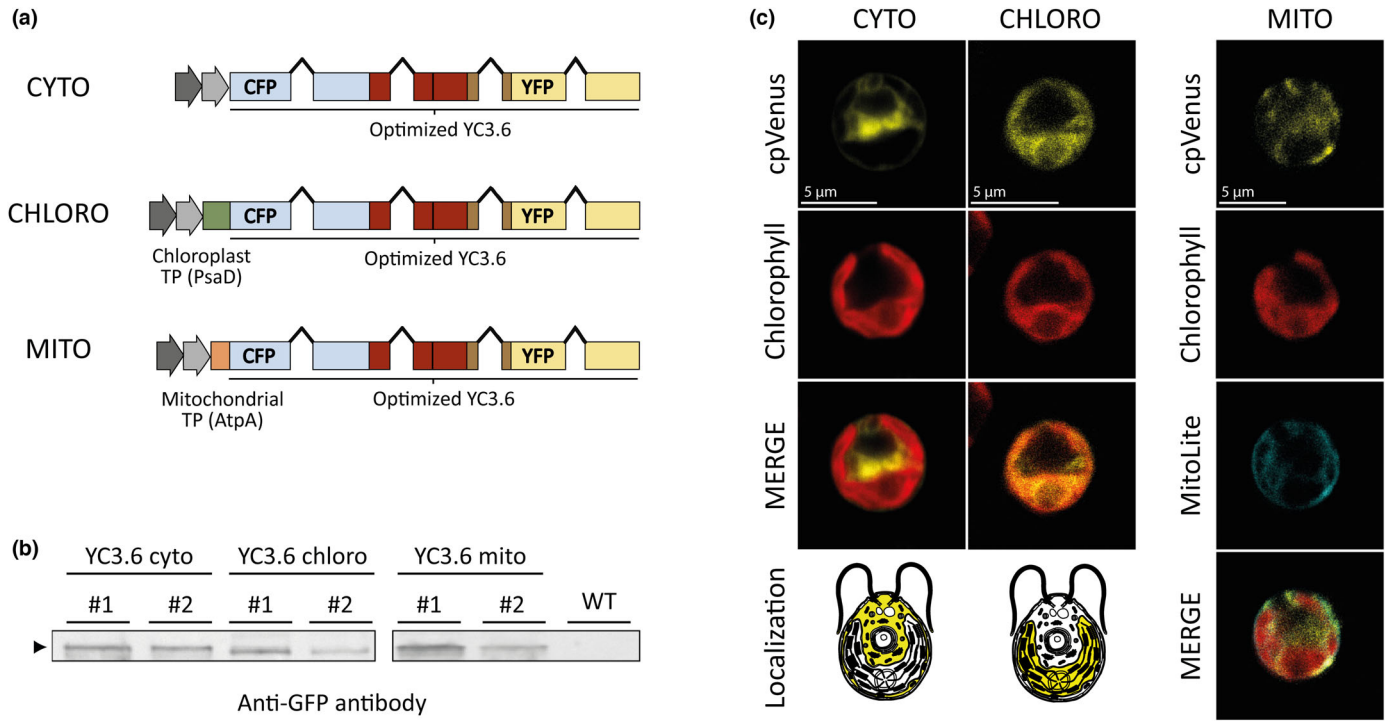

Fig. 1 YC3.6 expression, accumulation, and subcellular localization in *Chlamydomonas reinhardtii*. (a) Schematic representation of the expression vectors used for *C. reinhardtii* transformation with YC3.6. The 2546-bp coding region (exons shown as boxes), interrupted by the three Rbcs2 introns (thin lines), was synthesized with optimal *Chlamydomonas* codon usage. Different N-terminal targeting signals were inserted to target the sensors to the cytosol (CYTO), the chloroplast stroma (CHLORO), and the mitochondria (MITO). (b) Western blot analysis showing YC3.6 accumulation in transformant strains compared with the background strain UVM4 (UV-mediated mutant 4). (c) Representative confocal microscopy images of individual cells of the transformant lines selected. Shown are cpVenus (cpVenus) fluorescence, chlorophyll autofluorescence (Chlorophyll), MitoLite fluorescence (MitoLite), and all signals merged (MERGE). Localization panel shows schematic representations of a typical *C. reinhardtii* cell, highlighting in yellow the subcellular localization of the YC3.6 probe. UVM4 line herein used as a background strain does not harbor full and functional flagella.

stimulus from the 514 nm laser light did not induce significant [Ca^{2+}] increases at the level of all the three subcellular compartments (Fig. S5). Even so, the 514 nm line preferentially excite the cpVenus moiety of the YC3.6 probe, resulting in a positive change in the FRET ratio during the stimulation phase and likely bleaching fluorescence emission at high intensities. Accordingly, after-stimulus maximal FRET ratio change was significantly lower in all the three compartments at the higher intensities of light stimulation (Fig. S5). The stroma resting steady-state FRET ratio before the light stimulus was significantly lower in the chloroplast compared with the cytosol, indicating lower free Ca^{2+} concentrations (Fig. 2e). This is in accordance with what has been observed so far in plants for the relative stromal vs cytosolic [Ca^{2+}] (Sai & Johnson, 2002; Loro *et al.*, 2016).

Mitochondrial matrix steady-state level of FRET ratio was significantly higher than stroma, but still lower than cytosol, conversely to what have been shown in plant cells (Wagner *et al.*, 2015). A recent work in plant cells, however, reported comparable steady-state levels of FRET ratio between mitochondrial matrix and cytosolic compartments (Ruberti *et al.*, 2022). Intracellular Ca^{2+} dynamics were here monitored in *C. reinhardtii* UVM4 background cells (Neupert *et al.*, 2009), originally based on the cell wall-deficient, arginine prototrophic strain *cw15-302*, which has no flagella. *C. reinhardtii* flagella represent a highly dynamic and excitable signaling compartment, able to act in Ca^{2+} signaling either independently or in combination with the cell body (Collingridge *et al.*, 2013; Fort *et al.*, 2021). To investigate whether the presence of flagella is influencing light-dependent Ca^{2+} signaling, we expressed YC3.6 Ca^{2+} probe in a background strain bearing functional flagella (WT SAG73.72; Aiyar *et al.*, 2017). Subcellular localization of YC3.6 probe in the selected lines was confirmed by confocal microscopy (Fig. S6). The new YC3.6 expressing lines in WT SAG73.72 background were characterized by similar light-dependent chloroplast-specific [Ca^{2+}] elevations compared with the lines in UVM4 background, while in both backgrounds, no significant change in cytosolic or mitochondrial [Ca^{2+}] was detected (Fig. S6). To further dissect the link between the high light stimuli and the induced chloroplast Ca^{2+} *tran*sients, we evaluated the dose dependency of the response by using different laser light intensities (Fig. 3a,b). The chloroplast maximal FRET ratio variation and the time to reach maximal amplitude of FRET ratio correlate with the intensity of the stimulus applied, both using 633 nm or 405 nm laser lines (Fig. 3c,d). Treating the cells with increasing 633 nm light intensities, a proportional higher maximal amplitude of the response was obtained, while the time to reach the maximal FRET ratio values proportionally decreases (Fig. 3c). Ca^{2+}-signal amplitude and speed thus quantitatively reflect the intensity of

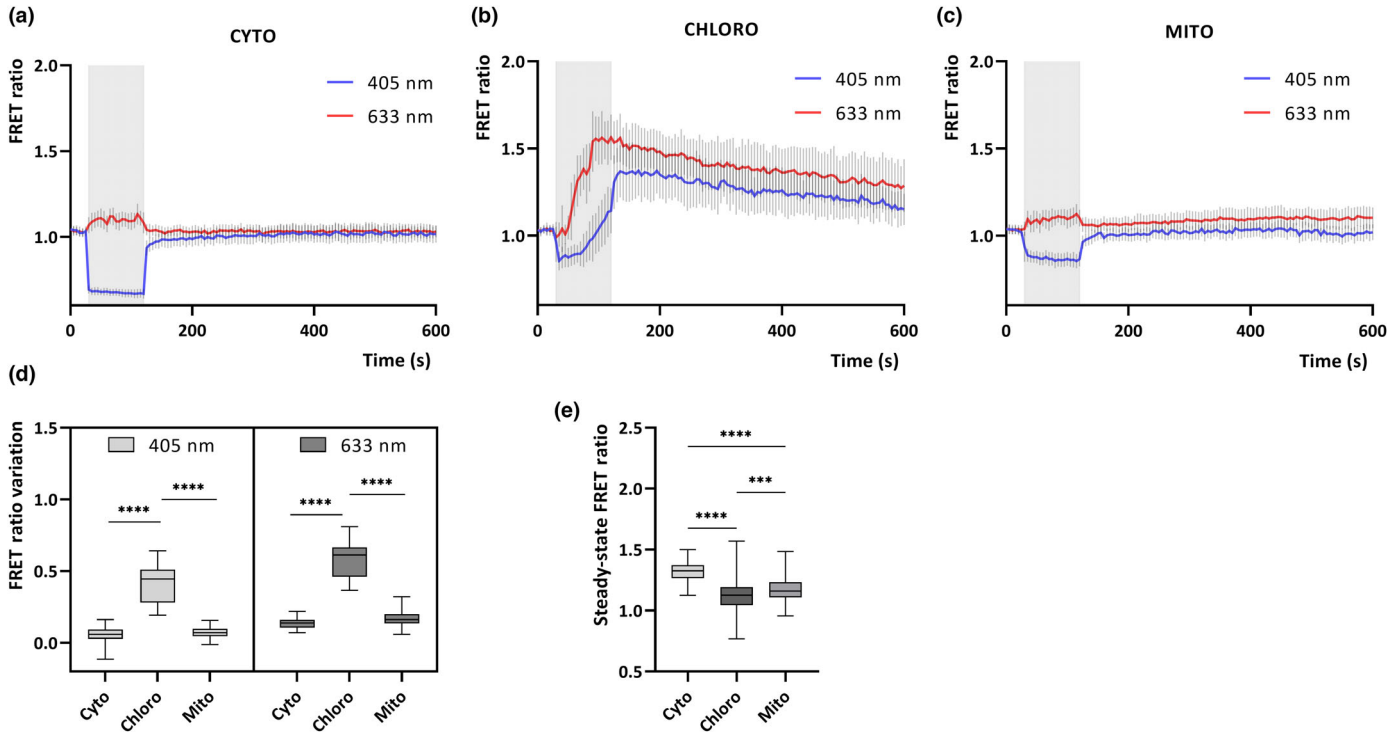

Fig. 2 Cytosolic, chloroplast, and mitochondrial Ca^{2+} dynamics in *Chlamydomonas reinhardtii* cells in response to high light stimuli. (a–c) Averaged and normalized FRET ratio ± SD of cytosolic (a, $n = 45$ cells), chloroplast (b, $n = 15$), and mitochondrial (c, $n = 41$ cells) YC3.6 in *C. reinhardtii* cells in response to high light stimuli (gray rectangle indicate the treatment, 90 s of 5 s^{-1} pulsed laser light, 405 nm 15% – 42 µW or 633 nm 75% – 550 µW). (d) Maximum FRET ratio variations triggered by light treatment at the level of the different subcellular compartments. Error bars indicate SD. (e) Basal steady-state FRET ratios at the level of the different subcellular compartments (averaged over a 25 s time before treatment, $n = 150$ cells). Error bars indicate SD. One-way ANOVA: ****, $P < 0.0001$; ***, $P < 0.001$.

the applied stress. 405 nm light-induced [Ca^{2+}] transient showed a weaker dose-dependence, with a trade-off at 7 µW, that was not triggering any significant Ca^{2+} transient (Fig. 3d) while maximum FRET ratio was obtained already with a light intensity of 20 µW. Taken together, these data suggest the presence of a clear dependency of the amplitude and kinetics of the chloroplast Ca^{2+} transient from the intensity of the light stimulus applied.

Light-induced chloroplast Ca^{2+} transients are influenced by high light acclimation and are partially dependent from photosynthetic activity

To investigate the origin of the high light-dependent stromal Ca^{2+} transient, its connection to extracellular Ca^{2+} availability was initially evaluated. Neither the depletion of extracellular [Ca^{2+}] by several consecutive washing steps (i.e. TAP medium without added $CaCl_2$) nor the treatment of the cells with the Ca^{2+} channel blocker $CoCl_2$ (Cho *et al.*, 1999) affected the stromal red high light-induced Ca^{2+} increase (Fig. 4a,b). Furthermore, the addition of the chelating agent EGTA to the external medium before measurements (as in Bickerton *et al.*, 2016) did not affect the light-induced Ca^{2+} response (Fig. S7). In all these cases, the chloroplast-specific Ca^{2+} transient remains unchanged and the maximum FRET ratio variation upon high light exposure was not distinguishable between control and treated cells (Figs 4b, S7). These results indicate that the observed stromal Ca^{2+} signature does not depend on extracellular sources of Ca^{2+}. Moreover, high light stimuli do not trigger any cytosolic [Ca^{2+}] variation that precedes the stromal Ca^{2+} increase (Fig. 2a), suggesting the presence of an organelle-autonomous response or the participation of other subcellular compartments as Ca^{2+} sources. To determine the molecular players at the base of high light-dependent chloroplast Ca^{2+} transients, the potential role of pigments and photosynthetic activity was investigated.

Chlorophyll molecules can absorb both blue and red wavelengths, and they might participate in the perception of light stimuli, thus being involved in the light-induced chloroplast Ca^{2+} signaling. Moreover, the photosynthetic process itself has a crucial role in the maintenance of the homeostasis of different ions across thylakoid membranes, indirectly regulating also [Ca^{2+}]. The trans-thylakoid pH gradient is indeed exploited not only for ATP production, but also for the import of Ca^{2+} into the lumen (Hochmal *et al.*, 2015). To assess the role of the photosynthetic machinery in the regulation of this chloroplast-specific Ca^{2+} response, we treated *C. reinhardtii* cells with specific photosynthetic electron transport inhibitors as DCMU, inhibiting PSII electron transport and thus linear electron flow, and DBMIB, inhibiting plastoquinone reduction and thus blocking both linear and cyclic electron flow (Uhmeyer *et al.*, 2017). Upon red light stimulation for 90 s, it was possible to observe that the inhibition of the photosynthetic electron transport, either with DCMU or with DBMIB, affects the chloroplast high light-induced Ca^{2+}

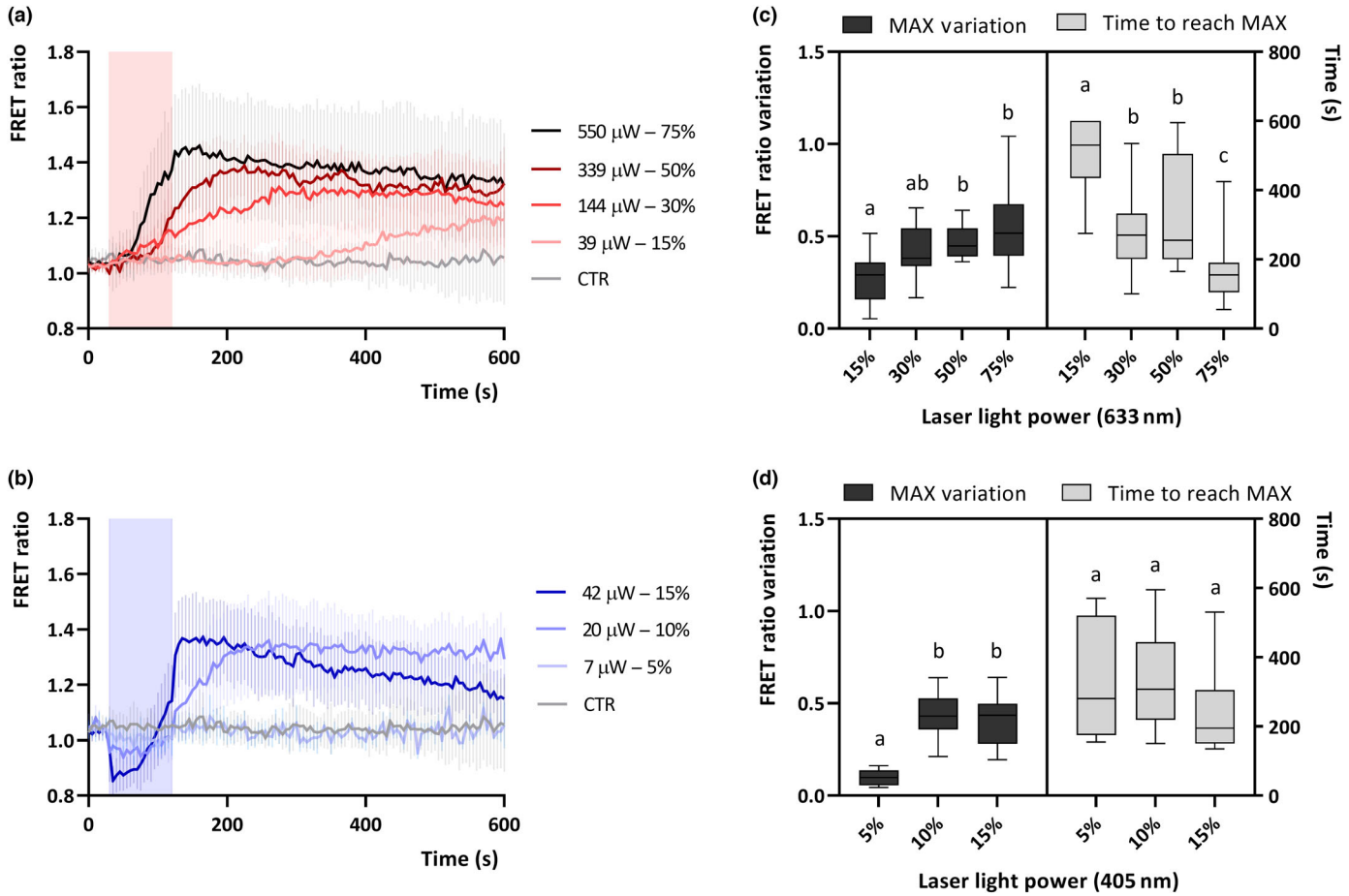

Fig. 3 Chloroplast Ca^{2+} transients in *Chlamydomonas reinhardtii in* response to different high light wavelengths and intensities. (a, b) Averaged and normalized FRET ratio ± SD of chloroplast YC3.6 in *C. reinhardtii* cells in response to different intensities of high light stimuli, 633 nm (a, $n > 13$ cells) and 405 nm (c, $n > 9$ cells; colored rectangle indicate the treatment, 90 s of 5 s^{-1} pulsed laser light, 633 nm or 405 nm at the indicated intensity). (c, d) Maximal FRET ratio variations and time to reach the maximum values, triggered by different high light treatments. Error bars indicate SD. Significantly different values are marked with different letters (a, b, c) as determined by One-way ANOVA ($P < 0.01$).

response only at the lower intensities of the applied red-light stimulus, namely 144 µW and 39 µW (30 and 15% of maximum laser power, respectively; Fig. 4c,d). In these cases, the maximal FRET ratio variation and the 'Area Under the Curve' (AUC, indicating both the amplitude and the duration of the Ca^{2+} transient) were significantly lower in the treated cells. At higher light intensities, when the photosynthetic electron transport is already saturated, the inhibitors were not significant. These results indicate a partial role of the photosynthetic apparatus and its physiological state in the onset of the chloroplast-specific Ca^{2+} response, triggered by high light stimulation.

The photosynthetic apparatus and the onset of light-dependent photosynthetic electron transport are modulated as a response to high light acclimation to minimize the harmful effects of an excessive irradiance, both on short and long time scales (Bonente *et al.*, 2012; Erickson *et al.*, 2015). To test whether high light acclimation could also influence the perception and response to light stimuli, affecting the high light-induced stromal Ca^{2+} transient, YC3.6 expressing lines were acclimated in photoautotrophy under high light irradiance (400 µmol photons m^{-1} s^{-2}). High light acclimated cells showed significantly lower resting stromal Ca^{2+} levels compared with cells grown in control light (Fig. 4e), reported as a lower resting steady-state FRET ratio. Moreover, when exposed to red high light treatment, high light acclimated cells displayed a significantly lower maximal FRET ratio variation of the induced chloroplast Ca^{2+} transient (Fig. 4f). These data suggest that an acclimation to high light condition can alter the chloroplast Ca^{2+}-mediated response to a high light stimulus. High light acclimation might indeed influence the perception of a light stimulus, change the chloroplast resting [Ca^{2+}], but also affect the pigment composition and the photosynthetic apparatus, mitigating the risk of saturation of electron transport flow upon high light exposure (Bonente *et al.*, 2012).

High light triggers H_2O_2 production in the chloroplast stroma that correlates with high light-induced Ca^{2+} transients

Reactive oxygen species, produced in the chloroplast as by-products of oxygenic photosynthesis, have been demonstrated as essential signaling molecules (Wakao & Niyogi, 2021; Foyer &

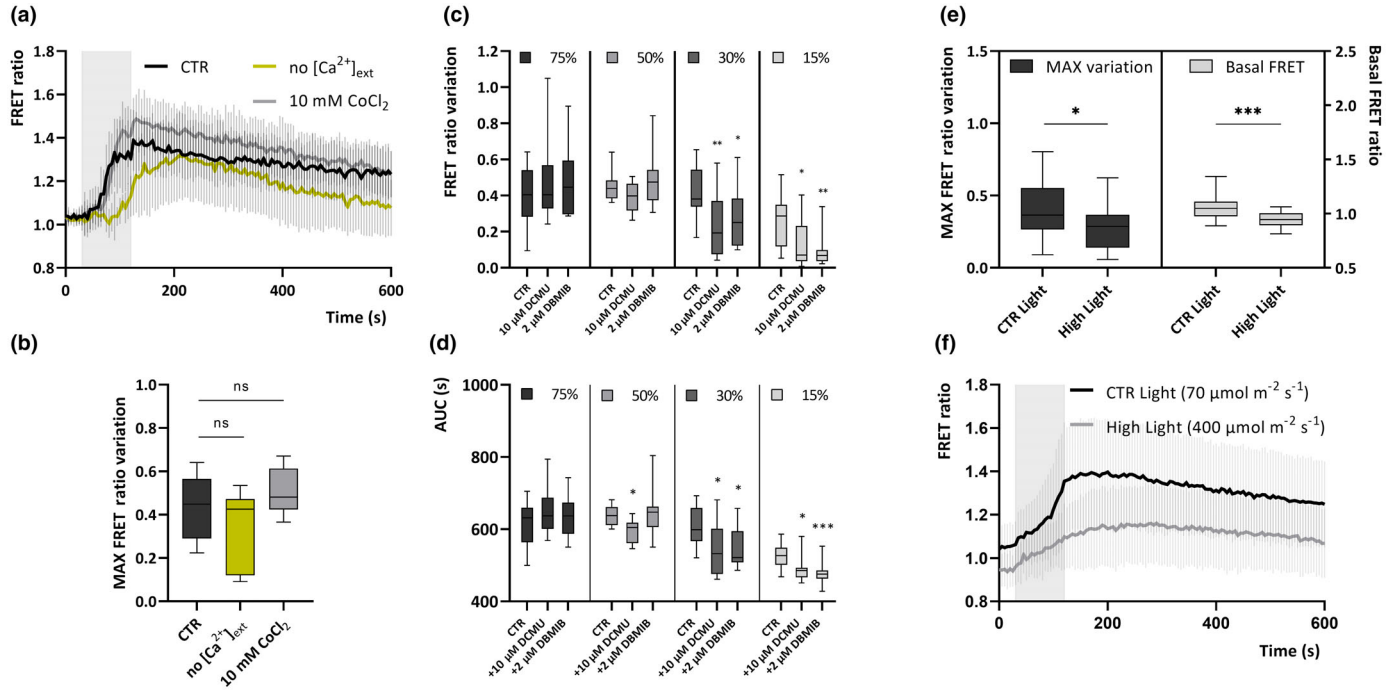

Fig. 4 Components of *Chlamydomonas reinhardtii* chloroplast Ca^{2+} dynamics in response to 633 nm high light stimulation. (a) Normalized FRET ratios ± SD of chloroplast YC3.6 in *C. reinhardtii* cells in response to 633 nm laser light stimulus (gray rectangle indicates the treatment, 90 s of 5 s^{-1} pulsed laser light at 550 µW – 75%). Black line represents the control, yellow line the cells depleted of external Ca^{2+}, and gray line the treatment with 10 mM $CoCl_2$ before the measurement ($n > 8$ cells). (b) Maximal FRET ratio variation upon stimulus and treatments explained in a. ($n > 8$ cells, one-way ANOVA: $P > 0.05$). (c, d) Maximal FRET ratio variation and AUC of FRET ratios in response to 633 nm laser light stimulus at the indicated intensities, control, and treatments with photosynthetic electron transport inhibitors (DCMU and DBMIB; $n > 12$ cells, one-way ANOVA: *, $P < 0.05$; **, $P < 0.01$; ***, $P < 0.001$). ns, not significantly different values. (e) Maximal FRET ratio variation (left) and basal steady-state FRET ratio before stimulus (right) upon conditions explained in (f). ($n = 22$ cells, Unpaired *t*-test: *, $P < 0.05$; ***, $P < 0.001$). (f) FRET ratios ± SD of chloroplast YC3.6 in *C. reinhardtii* cells autotrophically grown in control (black line) or high light (gray line) conditions, in response to 633 nm laser light stimulus (gray rectangle indicates the treatment, 90 s of 5 s^{-1} pulsed laser light at 550 µW – 75%). For all panels, error bars indicate SD.

Hanke, 2022). To test whether H_2O_2 levels within chloroplast stroma changed when the cells are exposed to our high light stimuli, we employed a cell line expressing the H_2O_2 sensor roGFP2-Tsa2ΔC_R in this subcellular compartment (Niemeyer *et al.*, 2021). We first confirmed the feasibility of H_2O_2 measurements with the stromal roGFP2-Tsa2ΔC_R sensor by monitoring in real time its reduction and oxidation in response to exogenously applied DTT and H_2O_2 respectively (Fig. S8). Similarly to what have been previously shown (Niemeyer *et al.*, 2021), we detected a decrease in the 405/488 nm ratio signal in response to DTT direct injection (reduction), followed by a ratio increase upon H_2O_2 treatment (oxidation). In accordance with what has been reported in previous experiments using whole-cell cultures exposed to high light (Niemeyer *et al.*, 2021), we observed in a real-time single-cell setup, stromal H_2O_2 levels increases following red (633 nm) high light exposure (Fig. 5a). The increase in stromal H_2O_2 levels exhibited a significant correlation with the intensity of the light treatment, increasing both the 405/488 nm ratio variation and the AUC of the traces at increasing light intensity (Fig. 5c). Red light induced also an increase in H_2O_2 levels in the cytosol (Fig. S9), as revealed using *C. reinhardtii* lines with roGFP2-Tsa2ΔC_R cytosolic localization (Niemeyer *et al.*, 2021). The effect of blue light could not be analyzed due to the direct absorption of the sensor in the 400–500 nm region.

Treating *C. reinhardtii* cells with DCMU or DBMIB significantly increased the chloroplast high light-induced H_2O_2 production, both at high and low 633 nm laser light intensities of the stimulus (Fig. S10). Accordingly, DCMU or DBMIB treatments were previously reported to strongly oxidize redox buffers in the chloroplast stroma of plant cells (Brunkard *et al.*, 2015). In addition, DCMU treatment significantly decreases the basal steady-state 405/488 nm ratio of the chloroplast stroma roGFP2-Tsa2ΔC_R in *C. reinhardtii* cells (Fig. S10), further indicating that blocking the photosynthetic electron transport can alter the chloroplast H_2O_2 production and homeostasis, differentially influencing the high light-induced H_2O_2 responses.

Interestingly, the effect of red light, increasing H_2O_2 in the chloroplasts, is positively correlated with the [Ca^{2+}] transients induced in the stroma by the same light stimuli (Fig. 5b): Both Ca^{2+} and H_2O_2 levels in the chloroplast showed significant increases upon high light treatment, proportional to the intensity of the applied stimulus. These results suggest a potential connection between the Ca^{2+} and H_2O_2 signaling systems in response to high light stimuli. To evaluate whether increased H_2O_2 could influence Ca^{2+} signaling, extracellular H_2O_2 concentration was increased to 1 mM by direct injection of a H_2O_2 solution to cells kept in the dark. In these conditions, a transient increase [Ca^{2+}] in the stromal YC3.6 expressing line could be observed even in

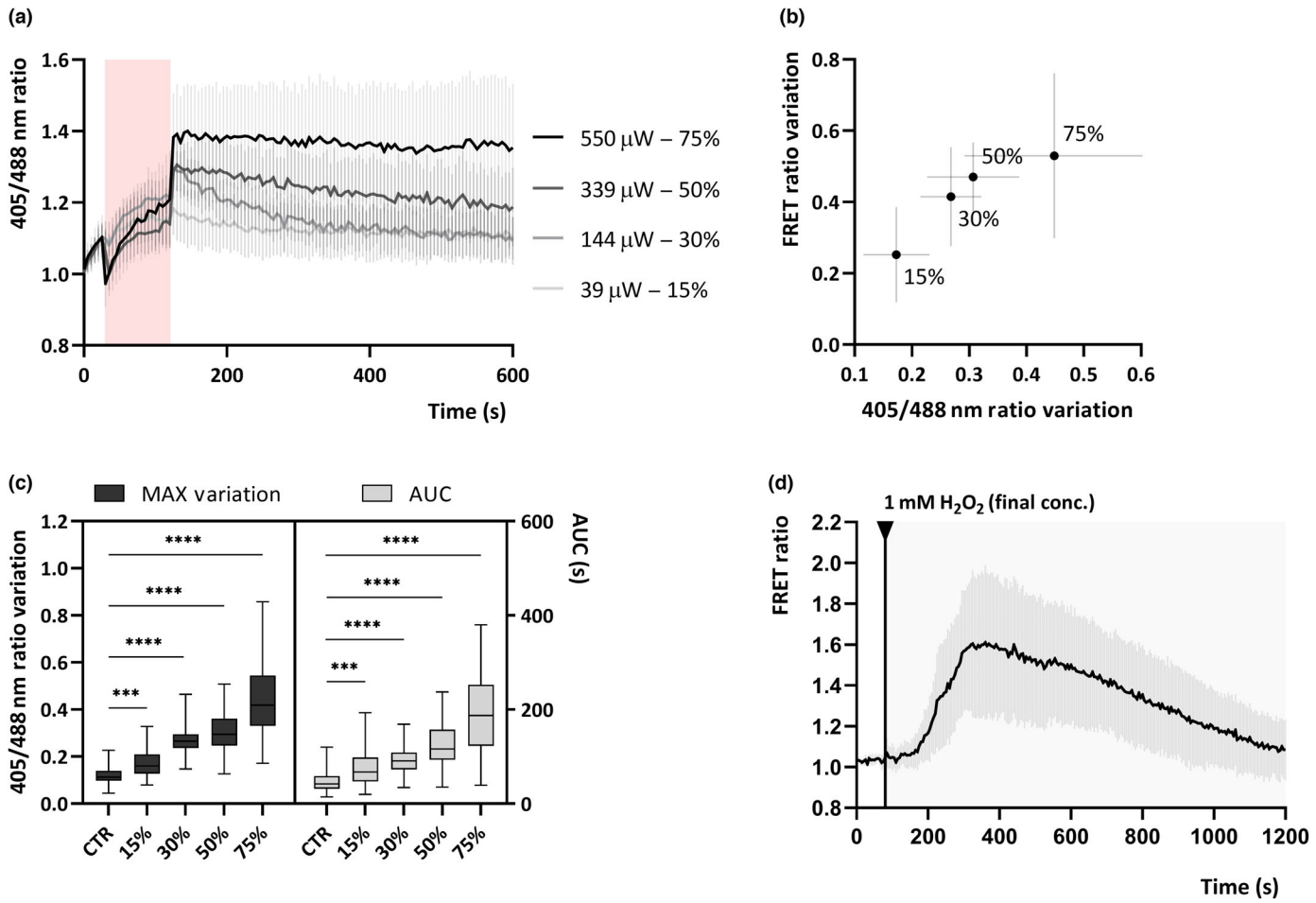

Fig. 5 Real-time single-cell monitoring of H_2O_2 levels in *Chlamydomonas reinhardtii* chloroplast stroma under high light exposure. (a) Normalized fluorescence measurement of roGFP2-Tsa2ΔC_R (as 405/488 nm ratio) after 633 nm laser light exposure at different intensities. The data are reported as means ± SD. Red rectangle indicates the treatment, 90 s of 5 s^{-1} pulsed laser light at the reported intensity. (b) Correlation between average maximal variation of FRET ratio (stromal YC3.6, *y*-axis) and 405/488 nm ratio (stromal roGFP2-Tsa2ΔC_R, *x*-axis) for each 633 nm laser intensity stimulation (Mean ± SD). (c) Maximal ratio variation and AUC of 405/488 nm ratios in response to 633 nm laser light stimulus (a) at the indicated intensities. Control (CTR) represents untreated cells. Error bars indicate SD ($n > 63$ cells, One-way ANOVA: ***, $P < 0.001$; ****, $P < 0.001$). (d) Normalized FRET ratio ± SD of chloroplast YC3.6 in *C. reinhardtii* cells in response to external H_2O_2 injection at the final concentration of 1 mM (black line at 80 s). $n = 7$ cells.

the absence of light stimuli (Fig. 5d). A H_2O_2-induced stromal [Ca^{2+}] transient has already been reported in *Arabidopsis* cell suspension cultures (Sello *et al.*, 2018), suggesting the presence of a conserved mechanism in *C. reinhardtii* in the response to an oxidative stress. An interplay between Ca^{2+} and ROS signaling might be present at the chloroplast level also in *C. reinhardtii* cells, potentially regulating the responses to high light stimuli.

The high light-induced stromal Ca^{2+} transient is significantly altered in *C. reinhardtii acry* mutant

Eukaryotic photosynthetic organisms have evolved different classes of light-sensitive receptors, among which cryptochromes (CRYs) and phototropins (PHOTs; Hegemann, 2008; Petersen *et al.*, 2021). In the case of *C. reinhardtii*, PHOT is a blue-light photoreceptor reported to be involved in several blue-light-dependent responses in *C. reinhardtii* (Huang & Beck, 2003; Petroutsos *et al.*, 2016), while the cryptochrome aCRY is the only photoreceptor known to be involved in red-light photoreception (Beel *et al.*, 2012; Greiner *et al.*, 2017). To investigate the possible involvement of photoreceptors in the high light-induced chloroplast Ca^{2+} transients, *phot* and *acry* mutants, with the respective wild-type background strains (WT CC-125 and WT SAG73.72; Petroutsos *et al.*, 2016; Greiner *et al.*, 2017), were engineered to express YC3.6 Ca^{2+} probe in the chloroplast. The chloroplast subcellular localization of YC3.6 probe in the selected lines was then confirmed by confocal microscopy (Fig. S11). Ca^{2+} imaging analysis on selected YC3.6 expressing lines for each different genetic background was performed in response to red (633 nm) and blue (405 nm) high light stimuli. *phot* mutant did not display any altered response to the applied high light stimuli compared with its background WT CC125 (Fig. 6a,b), excluding a possible contribution of PHOT protein in high light-induced Ca^{2+} transients. Interestingly, *acry* mutant showed a lowered high light-dependent stromal Ca^{2+} response compared with its background (WT SAG73.72) for

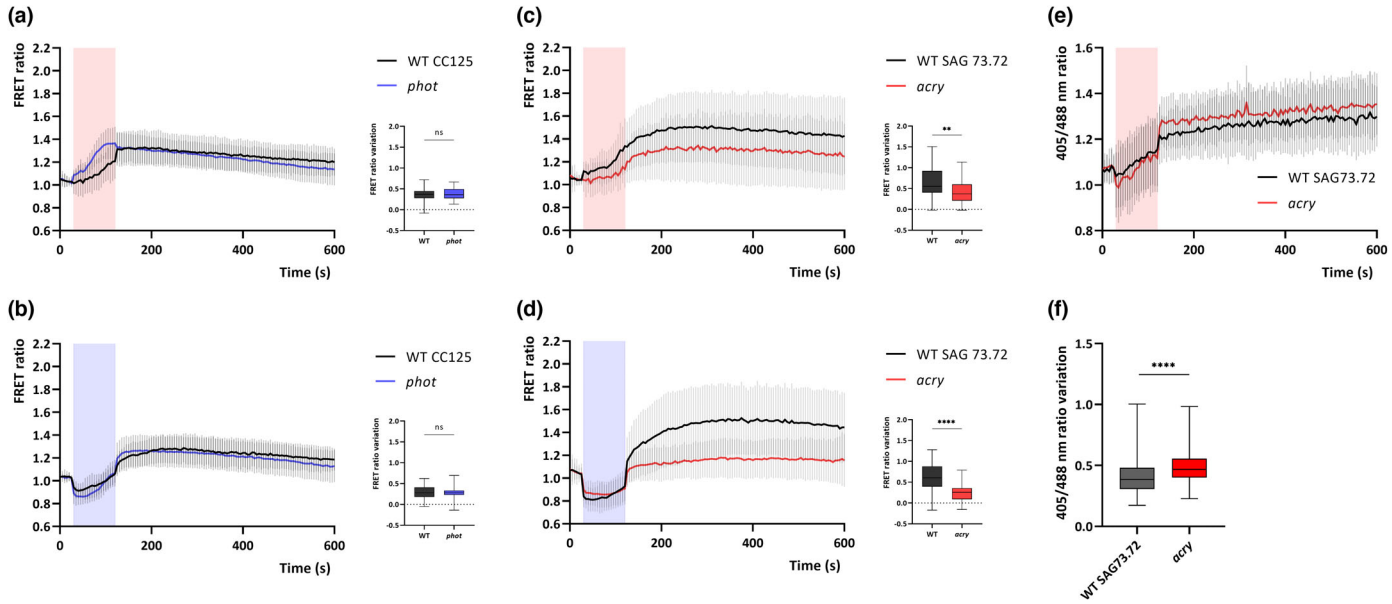

Fig. 6 Light-induced chloroplast Ca^{2+} and H_2O_2 transients in *Chlamydomonas reinhardtii phot* and *acry* mutants. Normalized chloroplast YC3.6 FRET ratio traces and Maximal FRET ratio variation distribution (right corner inset) of *C. reinhardtii* cells upon stimulation with 633 nm (a, c, 550 μW – 75%) and 405 nm (b, d, 42 μW – 15%) laser light (colored rectangles indicates the treatments, 90 s 5 s^{-1}). (a, b) FRET ratios ± SD of *phot* and wild-type background (WT CC125) cells ($n > 40$ cells). (c, d) FRET ratios ± SD of *acry* and wild-type background (WT SAG72.73) cells (c, $n > 40$ cells and d, $n > 57$). Results are reported as mean of at least 3 independent experiments. (e) Normalized fluorescence measurement of roGFP2-Tsa2ΔC_R (as 405/488 nm ratio) after 633 nm laser light exposure. The data are reported as means ± SD (red rectangle indicates the treatment, 90 s of 5 s^{-1} pulsed laser light at 550 μW – 75%). (f) Maximal variation of 405/488 nm ratios in response to 633 nm laser light stimulus (e, $n > 99$ cells). Unpaired *t*-test: **, $P < 0.01$; ****, $P < 0.0001$.

both red and blue-light stimuli tested (Fig. 6c,d), indicating an impairment but not a complete disruption of the light-induced stromal [Ca^{2+}] transient in this mutant line. These results suggest an important role for aCRY photoreceptor in mediating light-dependent Ca^{2+} signaling in *Chlamydomonas reinhardtii*. To better understand the molecular basis of *acry* impairment on light-dependent chloroplast Ca^{2+} signaling, different photosynthetic parameters were measured in *acry* mutant and compared with its background strain (Fig. S11) obtaining no significant differences, consistently with previous results (Petroutsos *et al.*, 2016). However, *acry* mutant, compared with its parental line, displayed significantly higher Chl *a* : *b* ratios in photoautotrophic conditions in control light and high light acclimated cells (Table S1). A slightly lower content of Chl(pg)/Cell in all the tested conditions was also observed, even if not with a significant difference. To investigate the potential role of aCRY in the high light-dependent H_2O_2 response, *acry* mutant and the respective background strain (WT SAG73.72) were engineered to express the roGFP2-Tsa2ΔC_R H_2O_2 sensor in the chloroplast. The subcellular localization of roGFP2-Tsa2ΔC_R in the selected lines was confirmed by confocal microscopy for one strain of each transgenic line (Fig. S12). *acry* mutant displayed even a slight increase of the chloroplast red light-induced H_2O_2 elevation compared with wild-type (Fig. 6e,f). These data exclude that the reduced light-induced chloroplast Ca^{2+} signaling observed in acry might be related to reduced photosynthetic activity or reduced H_2O_2 production, highlighting instead a different pigment content in the mutant, that might indirectly influence high light perception.

Discussion

In this work, *C. reinhardtii* lines stably expressing YC3.6 Ca^{2+} indicator at different subcellular localizations were generated to explore and dissect intracellular *in vivo* Ca^{2+} dynamics (Fig. 1). Light regulates chloroplast [Ca^{2+}] in plant cells, causing a stromal [Ca^{2+}] elevation upon dark transition (Sai & Johnson, 2002; Nomura *et al.*, 2012; Sello *et al.*, 2016, 2018), which is essential to modulate the activity of some Calvin cycle enzymes and inhibit CO_2 fixation during the night (Sai & Johnson, 2002). Here, our findings reveal a chloroplast Ca^{2+} transient elevation in response to high light stimulation in the green alga *C. reinhardtii* (Fig. 2) while no significant change in [Ca^{2+}] in the cytosolic and mitochondrial compartments was detected, suggesting the existence of a chloroplast-specific response. These results were obtained in UVM4 background, where flagella structures are not assembled; therefore, similar investigations were performed in a background strain bearing functional flagella (WT SAG73.72 background), confirming the results obtained in UVM4 background (Fig. S6). Chloroplast Ca^{2+} transients were triggered by both red and blue light, observing amplitude and kinetic properties related to the intensity of the applied stimuli (Fig. 3). The depletion of external Ca^{2+} or the treatment with a Ca^{2+} channel blocker did not affect the onset of the light-dependent chloroplast Ca^{2+} transients: similar independency from external Ca^{2+} was previously reported in the case of chloroplast Ca^{2+} transients measured in Arabidopsis plants expressing YC3.6 in the stroma (Loro *et al.*, 2016). These results, together with the absence of a

cytosolic Ca^{2+} response to light stimuli, lead to the hypothesis of a chloroplast-autonomous light-dependent Ca^{2+} response. In this model, thylakoid lumen might represent the main source for Ca^{2+} efflux in the stroma, even though other Ca^{2+} sources cannot be excluded, like the endoplasmic reticulum (ER), operating through chloroplast-ER membrane interaction domains (Pérez-Sancho *et al.*, 2016; Suzuki *et al.*, 2018). *C. reinhardtii* channelrhodopsin photoreceptors (ChR1 and ChR2) are green light-responsive ion channels localized in the plasma membrane above the eyespot, at the edge of the chloroplast, participating in the light-gated Ca^{2+}-dependent phototaxis mechanism (Nagel *et al.*, 2002, 2003; Berthold *et al.*, 2008; Pivato & Ballottari, 2021). No significant change in $[Ca^{2+}]$ in the three tested compartments was detected upon green light stimuli (Fig. S5), likely excluding the contribution of channelrhodopsins in the observed red or blue light-dependent chloroplast Ca^{2+} transients. However, it is also worth noting that YC3.6 is likely not suitable to monitor intracellular Ca^{2+} dynamics in response to green light, as it can selectively excite cpVenus moiety of the probe, causing its specific bleaching and ultimately compromising $[Ca^{2+}]$ measurements. Moreover, Ca^{2+} indicators with a higher sensitivity than YC3.6 could better reveal subtle Ca^{2+} increases that cannot be reported by the Cameleon indicator (Grenzi *et al.*, 2021). Thus, different Ca^{2+} probes should be considered in order to properly analyze the contribution of green light to light-dependent Ca^{2+} signals in *C. reinhardtii*.

Photosynthetic activity and light acclimation have a role in the shaping of the high light-induced chloroplast Ca^{2+} transients (Fig. 4): at the lower intensities of the light stimuli applied, significantly lower Ca^{2+} elevations were reported upon treatment with inhibitors of the photosynthetic electron transport chain (DCMU and DBMIB). Inhibitors of photosynthetic electron transport strongly affect the light-dependent proton import into lumen (Bonente *et al.*, 2012); thus, photosynthetic activity might have a role in the shaping of the Ca^{2+} chloroplast response, influencing ion homeostasis across thylakoid membranes and regulating also $[Ca^{2+}]$.

Consistently with this view, in high light acclimated cells, where light proton accumulation in the lumen is generally reduced (Bonente *et al.*, 2012), light-dependent Ca^{2+} transients were reduced (Fig. 4f). High light exposure over long time scales can induce in *C. reinhardtii* cells several adaptations, affecting the photosynthetic apparatus and light harvesting, altering pigment composition and antioxidant accumulation (Erickson *et al.*, 2015). The adaptation of the perception and photoprotective mechanisms to high light conditions might thus alter the perception of a high light stimulus, consequently lowering the induced stromal Ca^{2+} transient. However, the electrochemical proton gradient across thylakoid membranes is likely not the only possible trigger for Ca^{2+} chloroplast response, due to the similar Ca^{2+} transient observed at higher light intensity of the applied stimuli in presence or absence of the electron transport inhibitors DCMU and DBMIB.

By monitoring intracellular H_2O_2 levels at the single-cell level through the genetically encoded sensor roGFP2-Tsa2ΔC_R (Niemeyer *et al.*, 2021), it was possible to observe that chloroplast H_2O_2 production is enhanced upon high light stimulation, advancing the hypothesis of the presence of an interplay between Ca^{2+} and H_2O_2 signaling in this subcellular compartment (Fig. 5). As previously shown in plants, we reported in *C. reinhardtii* that an increase of extracellular H_2O_2 levels is causing a chloroplast Ca^{2+} increase, supporting the presence of an interplay at this level (Fig. 5d; Sello *et al.*, 2018). The positive correlation between stromal Ca^{2+} and H_2O_2 elevations, and light-independent chloroplast Ca^{2+} increase by treatment with external H_2O_2, suggest a molecular connection between H_2O_2 and Ca^{2+} signaling pathways that could be modulated by integrating molecules, such as ion channels or binding proteins. Plant annexins link ROS and cytosolic Ca^{2+} signaling but no annexins-like protein have been identified so far in *C. reinhardtii* (Jami *et al.*, 2012; Bickerton *et al.*, 2016). Alternatively, a plasma membrane-localized leucine-rich-repeat receptor kinase HPCA1 has been shown to mediate H_2O_2-induced activation of Ca^{2+} channels in guard cells (Richards *et al.*, 2014; Wu *et al.*, 2020); however, HPCA1 homologs could not be found up to now in *Chlamydomonas* genome. The *C. reinhardtii* chloroplast protein calredoxin might represent a further candidate, containing two domains to integrate Ca^{2+} and H_2O_2 signals, Ca^{2+}-sensing (four EF-hands) and TRX (Hochmal *et al.*, 2016). Future investigations in this direction might involve specific *C. reinhardtii* mutant lines for the candidate chloroplast Ca^{2+} ion channels/binding proteins or for the H_2O_2 generation/scavenging.

In *C. reinhardtii* cells, light can be perceived by photosynthetic pigments, including chlorophyll and carotenoid molecules, but also by specific photoreceptors. The Ca^{2+} response to both blue and red light was significantly altered in the absence of aCRY protein, the only photoreceptor that has been reported to our knowledge to respond to red or yellow light, in addition to blue light. Differently, the absence of PHOT did not influence chloroplast Ca^{2+} transients. *C. reinhardtii* aCRY is localized in the nucleus to a significant extent during the day in vegetative cells, but can be found throughout the cell body during the night and during gametogenesis (Zou *et al.*, 2017). aCRY participates in the cell cycle control, acting as a negative regulator for mating ability as well as for mating maintenance (Zou *et al.*, 2017); however, its role in the regulation of other light-dependent physiological processes has been poorly investigated. A direct role for aCRY in light-dependent chloroplast Ca^{2+} signaling could be based on the light-dependent activation of a signal transduction pathway, leading to the modulation of chloroplast Ca^{2+} concentration. Further research efforts are required to dissect the possible molecular components of this aCRY-dependent Ca^{2+} signal transduction pathway. Alternatively, an indirect role of aCRY could be proposed: The *acry* mutant indeed displays lowered transcript levels of some genes encoding components of the light-harvesting complex of photosynthesis (LHCBM6), as well as proteins involved in chlorophyll or carotenoid biosynthesis, upon red-light induction (Beel *et al.*, 2012, 2013). Accordingly, we reported a significantly higher Chl $a:b$ ratio in photoautotrophically grown *acry* cells, even if the photosynthetic parameters were not affected (Table S1; Fig. S11). Therefore, the lack of aCRY protein might indirectly affect light perception mechanisms in *C. reinhardtii* cells, influencing also the monitored high light-induced chloroplast Ca^{2+} responses. It should be considered that the *acry* strain, generated

with CRISPR/Cas9 technique, still shows small levels of aCRY protein in immunoblotting analysis (Greiner *et al.*, 2017). The presence of residual levels of aCRY protein might account for an incomplete impairment of the stromal Ca^{2+} response.

In summary, this work establishes a toolset to study Ca^{2+} dynamics at a subcellular level in *C. reinhardtii* cells and identifies a chloroplast-specific Ca^{2+} signaling response to light, which is positively related to the intensity of the applied stimuli. These findings demonstrate the role of intracellular Ca^{2+} signaling in the perception of the environment in green algae, suggesting the presence of conserved mechanisms among *Viridiplantae*, but also the existence of uncharacterized responses in *C. reinhardtii*, likely related to its unique Ca^{2+} signaling toolkit (Pivato & Ballottari, 2021). In *C. reinhardtii*, different triggers are involved in the light-induced signal transmission pathway that leads to chloroplast [Ca^{2+}] increase: saturation of the photosynthetic electron transport, that induces proton accumulation in the lumen and affects ion homeostasis, ROS formation and aCRY-dependent light perception. Additional work is required to understand whether these elements work in parallel or in series to each other: aCRY and ROS could modulate the light-dependent expression of photosynthetic genes and photosynthetic electron transport saturation could boost ROS formation. In conclusion, the findings herein reported provide new information on stress signaling in green algae and pave the way toward the investigation of chloroplast Ca^{2+} signaling and the dissection of its underlying molecular machinery.

Acknowledgements

We thank the Centro Piattaforme Tecnologiche (CPT) for providing access to the core facilities of the University of Verona and NOLIMITS, an advanced imaging facility established by the University of Milan. We thank Dr Dimitris Petroutsos (CNRS/CEA Grenoble) for providing *phot1* mutant and its background wild-type strain CC-125 mt+ and for helpful discussion on the results obtained. We thank Prof. Michael Schroda (Molecular Biotechnology & Systems Biology, TU Kaiserslautern, Germany) for providing transgenic roGFP2-Tsa2ΔC_R Chlamydomonas lines. We thank Prof. Glen Wheeler (Marine Biological Association, Plymouth, UK) for helpful and constructive discussion about the results herein presented. This work was supported by the research program 'Dipartimento di Eccellenza 2018–2022' (Ministero dell'Università e della Ricerca, DIPCEL5; to MP and MB), Piano di Sviluppo di Ateneo 2019 (University of Milan; to AC), and by a PhD fellowship from the University of Milan (to MG).

Competing interests

None declared.

Author contributions

MB and AC contributed to the conceptualization and supervision. AC, MG and MP contributed to the methodology. MP and MG contributed to the investigation. MP and MB contributed to the writing – original draft. MP, MB, AC and MG contributed to the writing – review and editing. AC and MB resources.

ORCID

Matteo Ballottari https://orcid.org/0000-0001-8410-3397
Alex Costa https://orcid.org/0000-0002-2628-1176
Matteo Grenzi https://orcid.org/0000-0003-2295-0018
Matteo Pivato https://orcid.org/0000-0002-1168-6357

Data availability

All the data herein described are included in Figures or in the Supporting Information. The strains here investigated are fully available upon request to the corresponding authors.

References

Aiyar P, Schaeme D, García-Altares M, Carrasco Flores D, Dathe H, Hertweck C, Sasso S, Mittag M. 2017. Antagonistic bacteria disrupt calcium homeostasis and immobilize algal cells. *Nature Communications* **8**: 1–13.

Baier T, Wichmann J, Kruse O, Lauersen KJ. 2018. Intron-containing algal transgenes mediate efficient recombinant gene expression in the green microalga *Chlamydomonas reinhardtii*. *Nucleic Acids Research* **46**: 6909–6919.

Baker NR. 2008. Chlorophyll fluorescence: a probe of photosynthesis *in vivo*. *Annual Review of Plant Biology* **59**: 89–113.

Beel B, Müller N, Kottke T, Mittag M. 2013. News about cryptochrome photoreceptors in algae. *Plant Signaling and Behavior* **8**: e22870.

Beel B, Prager K, Spexard M, Sasso S, Weiss D, Müller N, Heinnickel M, Dewez D, Ikoma D, Grossman AR *et al.* 2012. A flavin binding cryptochrome photoreceptor responds to both blue and red light in *Chlamydomonas reinhardtii*. *Plant Cell* **24**: 2992–3008.

Berthold P, Tsunoda SP, Ernst OP, Mages W, Gradmann D, Hegemanna P. 2008. Channelrhodopsin-1 initiates phototaxis and photophobic responses in Chlamydomonas by immediate light-induced depolarization. *Plant Cell* **20**: 1665–1677.

Bickerton P, Sello S, Brownlee C, Pittman JK, Wheeler GL. 2016. Spatial and temporal specificity of Ca^{2+} signalling in *Chlamydomonas reinhardtii* in response to osmotic stress. *New Phytologist* **212**: 920–933.

Bonente G, Pippa S, Castellano S, Bassi R, Ballottari M. 2012. Acclimation of *Chlamydomonas reinhardtii* to different growth irradiances. *Journal of Biological Chemistry* **287**: 5833–5847.

Brunkard JO, Runkel AM, Zambryski PC. 2015. Chloroplasts extend stromules independently and in response to internal redox signals. *Proceedings of the National Academy of Sciences, USA* **112**: 10044–10049.

Cho MR, Thatte HS, Silvia MT, Golan DE. 1999. Transmembrane calcium influx induced by ac electric fields. *FASEB Journal* **13**: 677–683.

Choi WG, Hilleary R, Swanson SJ, Kim SH, Gilroy S. 2016. Rapid, long-distance electrical and calcium signaling in plants. *Annual Review of Plant Biology* **67**: 287–307.

Collingridge P, Brownlee C, Wheeler GL. 2013. Compartmentalized calcium signaling in cilia regulates intraflagellar transport. *Current Biology* **23**: 2311–2318.

Costa A, Navazio L, Szabo I. 2018. The contribution of organelles to plant intracellular calcium signalling. *Journal of Experimental Botany* **69**: 4175–4193.

Croce R, Morosinotto T, Castelletti S, Breton J, Bassi R. 2002. The Lhca antenna complexes of higher plants photosystem I. *Biochimica et Biophysica Acta – Bioenergetics* **1556**: 29–40.

Demidchik V, Shabala S, Isayenkov S, Cuin TA, Pottosin I. 2018. Calcium transport across plant membranes: mechanisms and functions. *New Phytologist* **220**: 49–69.

Dodd AN, Kudla J, Sanders D. 2010. The language of calcium signaling. *Annual Review of Plant Biology* **61**: 593–620.

Edel KH, Marchadier E, Brownlee C, Kudla J, Hetherington AM. 2017. The evolution of calcium-based signalling in plants. *Current Biology* **27**: R667–R679.

Erickson E, Wakao S, Niyogi KK. 2015. Light stress and photoprotection in *Chlamydomonas reinhardtii*. *The Plant Journal* **82**: 449–465.

Fort C, Collingridge P, Brownlee C, Wheeler G. 2021. Ca^{2+} elevations disrupt interactions between intraflagellar transport and the flagella membrane in Chlamydomonas. *Journal of Cell Science* **134**: jcs253492.

Foyer CH, Hanke G. 2022. ROS production and signalling in chloroplasts: cornerstones and evolving concepts. *The Plant Journal* **111**: 642–661.

Greiner A, Kelterborn S, Evers H, Kreimer G, Sizova I, Hegemann P. 2017. Targeting of photoreceptor genes in *Chlamydomonas reinhardtii* via zinc-finger nucleases and CRISPR/Cas9. *Plant Cell* **29**: 2498–2518.

Grenzi M, Resentini F, Vanneste S, Zottini M, Bassi A, Costa A. 2021. Illuminating the hidden world of calcium ions in plants with a universe of indicators. *Plant Physiology* **187**: 550–571.

Harris E. 2008. *The Chlamydomonas sourcebook: introduction into Chlamydomonas and its laboratory use*. Cambridge, MA, USA: Academic Press.

Hegemann P. 2008. Algal sensory photoreceptors. *Annual Review of Plant Biology* **59**: 167–189.

Hochmal AK, Schulze S, Trompelt K, Hippler M. 2015. Calcium-dependent regulation of photosynthesis. *Biochimica et Biophysica Acta* **1847**: 993–1003.

Hochmal AK, Zinzius K, Charoenwattanasatien R, Gäbelein P, Mutoh R, Tanaka H, Schulze S, Liu G, Scholz M, Nordhues A *et al.* 2016. Calredoxin represents a novel type of calcium-dependent sensor-responder connected to redox regulation in the chloroplast. *Nature Communications* **7**: 1–14.

Hou Y, Bando Y, Carrasco Flores D, Hotter V, Das R, Schiweck B, Melzer T, Arndt HD, Mittag M. 2023. A cyclic lipopeptide produced by an antagonistic bacterium relies on its tail and transient receptor potential-type Ca^{2+} channels to immobilize a green alga. *New Phytologist* **237**: 1620–1635.

Huang K, Beck CF. 2003. Phototropin is the blue-light receptor that controls multiple steps in the sexual life cycle of the green alga *Chlamydomonas reinhardtii*. *Proceedings of the National Academy of Sciences, USA* **100**: 6269–6274.

Jami SK, Clark GB, Ayele BT, Ashe P, Kirti PB. 2012. Genome-wide comparative analysis of annexin superfamily in plants. *PLoS ONE* **7**: e47801.

Kindle KL. 1990. High-frequency nuclear transformation of *Chlamydomonas reinhardtii*. *Proceedings of the National Academy of Sciences, USA* **87**: 1228–1232.

van Kooten O, Snel JFH. 1990. The use of chlorophyll fluorescence nomenclature in plant stress physiology. *Photosynthesis Research* **25**: 147–150.

Kropat J, Hong-Hermesdorf A, Casero D, Ent P, Castruita M, Pellegrini M, Merchant SS, Malasarn D. 2011. A revised mineral nutrient supplement increases biomass and growth rate in *Chlamydomonas reinhardtii*. *The Plant Journal* **66**: 770–780.

Kudla J, Becker D, Grill E, Hedrich R, Hippler M, Kummer U, Parniske M, Romeis T, Schumacher K. 2018. Advances and current challenges in calcium signaling. *New Phytologist* **218**: 414–431.

Laemmli UK. 1970. Cleavage of structural proteins during the assembly of the head of bacteriophage T4. *Nature* **227**: 680–685.

Lauersen KJ, Kruse O, Mussgnug JH. 2015. Targeted expression of nuclear transgenes in *Chlamydomonas reinhardtii* with a versatile, modular vector toolkit. *Applied Microbiology and Biotechnology* **99**: 3491–3503.

Lenzoni G, Knight MR. 2019. Increases in absolute temperature stimulate free calcium concentration elevations in the chloroplast. *Plant and Cell Physiology* **60**: 538–548.

Loro G, Costa A. 2013. Imaging of mitochondrial and nuclear Ca^{2+} dynamics in arabidopsis roots. *Cold Spring Harbor Protocols* **2013**: 781–785.

Loro G, Wagner S, Doccula FG, Behera S, Weinl S, Kudla J, Schwarzländer M, Costa A, Zottini M. 2016. Chloroplast-specific *in vivo* Ca^{2+} imaging using Yellow Cameleon fluorescent protein sensors reveals organelle-autonomous Ca^{2+} signatures in the stroma. *Plant Physiology* **171**: 2317–2330.

Martí Ruiz MC, Jung HJ, Webb AAR. 2020. Circadian gating of dark-induced increases in chloroplast- and cytosolic-free calcium in Arabidopsis. *New Phytologist* **225**: 1993–2005.

Morgan B, Sobotta MC, Dick TP. 2011. Measuring EGSH and H_2O_2 with roGFP2-based redox probes. *Free Radical Biology & Medicine* **51**: 1943–1951.

Morgan B, Van Laer K, Owusu TNE, Ezeriņa D, Pastor-Flores D, Amponsah PS, Tursch A, Dick TP. 2016. Real-time monitoring of basal H_2O_2 levels with peroxiredoxin-based probes. *Nature Chemical Biology* **12**: 437–443.

Nagai T, Yamada S, Tominaga T, Ichikawa M, Miyawaki A. 2004. Expanded dynamic range of fluorescent indicators for Ca^{2+} by circularly permuted yellow fluorescent proteins. *Proceedings of the National Academy of Sciences, USA* **101**: 10554–10559.

Nagel G, Ollig D, Fuhrmann M, Kateriya S, Musti AM, Bamberg E, Hegemann P. 2002. Channelrhodopsin-1: a light-gated proton channel in green algae. *Science* **296**: 2395–2398.

Nagel G, Szellas T, Huhn W, Kateriya S, Adeishvili N, Berthold P, Ollig D, Hegemann P, Bamberg E. 2003. Channelrhodopsin-2, a directly light-gated cation-selective membrane channel. *Proceedings of the National Academy of Sciences, USA* **100**: 13940–13945.

Navazio L, Formentin E, Cendron L, Szabò I. 2020. Chloroplast calcium signaling in the spotlight. *Frontiers in Plant Science* **11**: 186.

Neupert J, Karcher D, Bock R. 2009. Generation of Chlamydomonas strains that efficiently express nuclear transgenes. *The Plant Journal* **57**: 1140–1150.

Niemeyer J, Scheuring D, Oestreicher J, Morgan B, Schroda M. 2021. Real-time monitoring of subcellular H_2O_2 distribution in *Chlamydomonas reinhardtii*. *Plant Cell* **33**: 2935–2949.

Nomura H, Komori T, Uemura S, Kanda Y, Shimotani K, Nakai K, Furuichi T, Takebayashi K, Sugimoto T, Sano S *et al.* 2012. Chloroplast-mediated activation of plant immune signalling in Arabidopsis. *Nature Communications* **3**: 910–926.

Pérez-Sancho J, Tilsner J, Samuels AL, Botella MA, Bayer EM, Rosado A. 2016. Stitching organelles: organization and function of specialized membrane contact sites in plants. *Trends in Cell Biology* **26**: 705–717.

Petersen J, Rredhi A, Szyttenholm J, Oldemeyer S, Kottke T, Mittag M. 2021. The world of algae reveals a broad variety of cryptochrome properties and functions. *Frontiers in Plant Science* **12**: 2472.

Petroutsos D. 2017. Chlamydomonas photoreceptors: cellular functions and impact on physiology. In: Hippler M, ed. *Chlamydomonas: biotechnology and biomedicine. Microbiology Monographs, vol. 31*. Cham, Switzerland: Springer, 1–19.

Petroutsos D, Busch A, Janßen I, Trompelt K, Bergner SV, Weinl S, Holtkamp M, Karst U, Kudla J, Hippler M. 2011. The chloroplast calcium sensor CAS is required for photoacclimation in *Chlamydomonas reinhardtii*. *Plant Cell* **23**: 2950–2963.

Petroutsos D, Tokutsu R, Maruyama S, Flori S, Greiner A, Magneschi L, Cusant L, Kottke T, Mittag M, Hegemann P *et al.* 2016. A blue-light photoreceptor mediates the feedback regulation of photosynthesis. *Nature* **537**: 563–566.

Pirayesh N, Giridhar M, Ben Khedher A, Vothknecht UC, Chigri F. 2021. Organellar calcium signaling in plants: an update. *Biochimica et Biophysica Acta (BBA) – Molecular Cell Research* **1868**: 118948.

Pivato M, Ballottari M. 2021. *Chlamydomonas reinhardtii* cellular compartments and their contribution to intracellular calcium signalling. *Journal of Experimental Botany* **72**: 5312–5335.

Quarmby LM, Hartzell HC. 1994. Two distinct, calcium-mediated, signal transduction pathways can trigger deflagellation in *Chlamydomonas reinhardtii*. *Journal of Cell Biology* **124**: 807–815.

Resentini F, Grenzi M, Ancora D, Cademartori M, Luoni L, Franco M, Bassi A, Bonza MC, Costa A. 2021a. Simultaneous imaging of ER and cytosolic Ca^{2+} dynamics reveals long-distance ER Ca^{2+} waves in plants. *Plant Physiology* **187**: 603–617.

Resentini F, Ruberti C, Grenzi M, Bonza MC, Costa A. 2021b. The signatures of organellar calcium. *Plant Physiology* **187**: 1985–2004.

Richards SL, Laohavisit A, Mortimer JC, Shabala L, Swarbreck SM, Shabala S, Davies JM. 2014. Annexin 1 regulates the H_2O_2-induced calcium signature in *Arabidopsis thaliana* roots. *The Plant Journal* **77**: 136–145.

Rocha AG, Vothknecht UC. 2012. The role of calcium in chloroplasts–an intriguing and unresolved puzzle. *Protoplasma* **249**: 957–966.

Rose MM, Scheer D, Hou Y, Hotter VS, Komor AJ, Aiyar P, Scherlach K, Vergara F, Yan Q, Loper JE *et al.* 2021. The bacterium Pseudomonas protegens antagonizes the microalga *Chlamydomonas reinhardtii* using a blend of toxins. *Environmental Microbiology* **23**: 5525–5540.

Ruberti C, Feitosa-Araujo E, Xu Z, Wagner S, Grenzi M, Darwish E, Lichtenauer S, Fuchs P, Parmagnani AS, Balcerowicz D *et al.* 2022. MCU proteins dominate *in vivo* mitochondrial Ca^{2+} uptake in Arabidopsis roots. *Plant Cell* **34**: 4428–4452.

Sai J, Johnson CH. 2002. Dark-stimulated calcium ion fluxes in the chloroplast stroma and cytosol. *Plant Cell* **14**: 1279–1291.

Sello S, Moscatiello R, Mehlmer N, Leonardelli M, Carraretto L, Cortese E, Zanella FG, Baldan B, Szabò I, Vothknecht UC. 2018. Chloroplast Ca^{2+} fluxes into and across thylakoids revealed by thylakoid-targeted aequorin probes. *Plant Physiology* **177**: 38–51.

Sello S, Perotto J, Carraretto L, Szabò I, Vothknecht UC, Navazio L. 2016. Dissecting stimulus-specific Ca^{2+} signals in amyloplasts and chloroplasts of *Arabidopsis Thaliana* cell suspension cultures. *Journal of Experimental Botany* **67**: 3965–3974.

Stael S, Wurzinger B, Mair A, Mehlmer N, Vothknecht UC, Teige M. 2012. Plant organellar calcium signalling: an emerging field. *Journal of Experimental Botany* **63**: 1525–1542.

Suzuki N, Koussevitzky S, Mittler R, Miller G. 2012. ROS and redox signalling in the response of plants to abiotic stress. *Plant, Cell & Environment* **35**: 259–270.

Suzuki R, Nishii I, Okada S, Noguchi T. 2018. 3D reconstruction of endoplasmic reticulum in a hydrocarbon-secreting green alga, *Botryococcus braunii* (Race B). *Planta* **247**: 663–677.

Terashima M, Petroutsos D, Hüdig M, Tolstygina I, Trompelt K, Gäbelein P, Fufezan C, Kudla J, Weinl S, Finazzi G *et al.* 2012. Calcium-dependent regulation of cyclic photosynthetic electron transfer by a CAS, ANR1, and PGRL1 complex. *Proceedings of the National Academy of Sciences, USA* **109**: 17717–17722.

Uhmeyer A, Cecchin M, Ballottari M, Wobbe L. 2017. Impaired mitochondrial transcription termination disrupts the stromal redox poise in chlamydomonas. *Plant Physiology* **174**: 1399–1419.

Verret F, Wheeler G, Taylor AR, Farnham G, Brownlee C. 2010. Calcium channels in photosynthetic eukaryotes: implications for evolution of calcium-based signalling. *New Phytologist* **187**: 23–43.

Volkner C, Holzner LJ, Day PM, Ashok AD, De Vries J, Bolter B, Kunz HH. 2021. Two plastid POLLUX ion channel-like proteins are required for stress-triggered stromal Ca^{2+} release. *Plant Physiology* **187**: 2110–2125.

Wagner S, Behera S, De Bortoli S, Logan DC, Fuchs P, Carraretto L, Teardo E, Cendron L, Nietzel T, Füßl M *et al.* 2015. The EF-Hand Ca^{2+} binding protein MICU choreographs mitochondrial Ca^{2+} dynamics in Arabidopsis. *Plant Cell* **27**: 3190–3212.

Wakabayashi K, Ide T, Kamiya R. 2009. Calcium-dependent flagellar motility activation in *Chlamydomonas reinhardtii* in response to mechanical agitation. *Cell Motility and the Cytoskeleton* **66**: 736–742.

Wakao S, Niyogi KK. 2021. Chlamydomonas as a model for reactive oxygen species signaling and thiol redox regulation in the green lineage. *Plant Physiology* **187**: 687–698.

Wheeler GL. 2017. *Calcium-dependent signalling processes in Chlamydomonas.* Cham, Germany: Springer, 233–255.

Wheeler GL, Joint I, Brownlee C. 2007. Rapid spatiotemporal patterning of cytosolic Ca^{2+} underlies flagellar excision in *Chlamydomonas reinhardtii*. *The Plant Journal* **53**: 401–413.

Wu F, Chi Y, Jiang Z, Xu Y, Xie L, Huang F, Wan D, Ni J, Yuan F, Wu X *et al.* 2020. Hydrogen peroxide sensor HPCA1 is an LRR receptor kinase in Arabidopsis. *Nature* **578**: 577–581.

Yang Y, Costa A, Leonhardt N, Siegel RS, Schroeder JI. 2008. Isolation of a strong Arabidopsis guard cell promoter and its potential as a research tool. *Plant Methods* **4**: 6.

Zou Y, Wenzel S, Müller N, Prager K, Jung EM, Kothe E, Kottke T, Mittag M. 2017. An animal-like cryptochrome controls the Chlamydomonas sexual cycle. *Plant Physiology* **174**: 1334–1347.

Supporting Information

Additional Supporting Information may be found online in the Supporting Information section at the end of the article.

Fig. S1 Laser power used to expose *Chlamydomonas reinhardtii* cells to light stimuli.

Fig. S2 YC3.6 protein accumulation in *Chlamydomonas reinhardtii* and influence on PSII quantum yield (PSIIΦ).

Fig. S3 Compartment-specific Ca^{2+} dynamics in *Chlamydomonas reinhardtii* cells treated with $CaCl_2$.

Fig. S4 Chloroplast Ca^{2+} dynamics in a *Chlamydomonas reinhardtii* cell in response to high light stimulus.

Fig. S5 Cytosolic, chloroplast, and mitochondrial Ca^{2+} dynamics in *Chlamydomonas reinhardtii* cells in response to green high light stimuli.

Fig. S6 Cytosolic, chloroplast, and mitochondrial Ca^{2+} dynamics in *Chlamydomonas reinhardtii* WT SAG73.72 cells in response to high light stimuli.

Fig. S7 Chloroplast Ca^{2+} dynamics in response to 633 nm high light stimulation in *Chlamydomonas reinhardtii*: external [Ca^{2+}] independency.

Fig. S8 Real-time single-cell monitoring of H_2O_2 levels in *Chlamydomonas reinhardtii* chloroplast stroma after exogenous DTT and H_2O_2 treatments.

Fig. S9 Real-time single-cell monitoring of H_2O_2 levels in *Chlamydomonas reinhardtii* cytosol and chloroplast stroma under high light exposure.

Fig. S10 Real-time single-cell monitoring of H_2O_2 levels in the *Chlamydomonas reinhardtii* chloroplast stroma under high light exposure and DCMU or DBMIB treatments.

Fig. S11 Photosynthetic parameters of *Chlamydomonas reinhardtii* WT SAG73.72 and *acry* cells.

Fig. S12 Chloroplast targeting of YC3.6 and roGFP2-Tsa2ΔC_R proteins in different *Chlamydomonas reinhardtii* lines.

Table S1 Pigment analysis on *Chlamydomonas reinhardtii* WT SAG73.72 and *acry* strains.

Please note: Wiley is not responsible for the content or functionality of any Supporting Information supplied by the authors. Any queries (other than missing material) should be directed to the *New Phytologist* Central Office.